Cross-Section Fluctuations in Chaotic Scattering

B. Dietz[a], H. L. Harney[b], A. Richter[*,a,c], F. Schäfer[a], H. A. Weidenmüller[b]

[a] *Institut für Kernphysik, Technische Universität Darmstadt, D-64289 Darmstadt, Germany*
[b] *Max-Planck-Institut für Kernphysik, D-69029 Heidelberg, Germany*
[c] *ECT*, Villa Tambosi, I-38100 Villazzano (Trento), Italy*

Abstract

For the theoretical prediction of cross–section fluctuations in chaotic scattering, the cross-section autocorrelation function is needed. That function is not known analytically. Using experimental data and numerical simulations, we show that an analytical approximation to the cross-section autocorrelation function can be obtained with the help of expressions first derived by Davis and Boosé. Given the values of the average S–matrix elements and the mean level density of the scattering system, one can then reliably predict cross-section fluctuations.

1. Purpose

Quantum chaotic scattering is an ubiquitous phenomenon. It occurs, for instance, in nuclear physics [1], in electron transport through disordered mesoscopic samples [2], and in microwave billiards [3]. In all cases, the cross section displays random fluctuations versus energy or frequency. These are due to the random features of the underlying resonances. With d the average resonance spacing and Γ the average width, data on cross-section fluctuations exist for the entire range of the parameter Γ/d, from the regime of isolated resonances ($\Gamma \ll d$) to that of strongly overlapping resonances ($\Gamma \gg d$). The analysis of the data focuses on the value of the average cross section and on quantities that characterize the cross-section fluctuations. These are the variance of the cross section and certain correlation functions. For the analysis, one needs theoretical expressions for these quantities. These should be generic and only use a minimum of adjustable parameters.

The generic theoretical treatment of chaotic scattering employs a combination of scattering theory and random-matrix theory [1] and uses as input the values of d and of the energy-averaged elements $\overline{S}$ of the scattering matrix S. Analytical results exist for the S-matrix autocorrelation and cross-correlation functions [1] (including the value of the average cross section) and for the third and fourth moments of the S-matrix [4, 5]. Because of the complexity of the problem, analytical results for higher moments of the cross section or for cross-section correlation functions cannot be expected in the foreseeable future.

The present paper aims at filling that gap. We combine the available analytical information [1, 4, 5], results of computer simulations, and of experimental work on microwave billiards [3, 6] to study the cross-section autocorrelation function for all values of Γ/d. In particular, we address the following questions. (i) For which values of Γ/d and with which accuracy can the cross-section autocorrelation function be predicted in terms of the S-matrix autocorrelation function? (ii) Which analytical alternatives exist should that approach fail?

2. Framework

We consider chaotic scattering in a time-reversal invariant system described by a unitary and symmetric scattering matrix $S_{ab}(E)$. Here $a, b = 1, \ldots, \Lambda$ denote the channels and E the energy (or, in the case of microwave billiards, the frequency). The number Λ of channels may range from unity to a large number, $\Lambda \gg 1$. Chaotic scattering is modeled by writing the S-matrix in the form [7]

$$S_{ab}(E) = \delta_{ab} - i \sum_{\mu} W_{a\mu} D^{-1}_{\mu\nu}(E) W_{b\nu} \qquad (1)$$

where

$$D_{\mu\nu}(E) = E\,\delta_{\mu\nu} - H_{\mu\nu} + i\pi \sum_{c} W_{c\mu} W_{c\nu} \; . \qquad (2)$$

The real and symmetric Hamiltonian matrix H has dimension $N \gg 1$ and describes the dynamics of N resonances labeled by Greek letters. These are coupled to the channels by the real matrix elements $W_{a\mu}$. Chaos is taken into account by choosing H as a member of the Gaussian orthogonal ensemble (GOE) of random matrices [1]. Thus, the elements of H are Gaussian random variables with zero mean values and second moments given by $\overline{H_{\mu\nu} H_{\rho\sigma}} = (\lambda^2/N)[\delta_{\mu\rho}\delta_{\nu\sigma} + \delta_{\mu\sigma}\delta_{\nu\rho}]$. Here and in the sequel, the overbar denotes the average over the ensemble. The parameter λ determines (or is determined by) the average level spacing d of the N resonances. It is convenient to decompose $S(E)$ into an average and a fluctuating part,

$$S_{ab}(E) = \overline{S_{aa}}\;\delta_{ab} + S^{\rm fl}_{ab}(E) \; , \qquad (3)$$

*Corresponding author
Email address: richter@ikp.tu-darmstadt.de (A. Richter)

where the average S-matrix $\overline{S}$ is assumed to be diagonal. The values of the diagonal elements $\overline{S_{aa}}$ serve as input parameters for the statistical model and are assumed to be known. That is the typical case: In nuclei, $\overline{S_{aa}}$ is given in terms of the optical model of elastic scattering, in microwave billiards $\overline{S_{aa}}$ is determined by the running average over a measured spectrum [3, 6]. In rare cases, the average S-matrix may not be diagonal. By an orthogonal transformation in channel space, $\overline{S}$ can be reduced to diagonal form, see Refs. [5, 8]. For simplicity we do not address that case. By the same transformation, the phases of the S-matrix usually appearing as factors on the right–hand side of Eq. (3), can be removed. Both for the S-matrix model Eq. (1) considered in the present work and the experimental data the average S-matrix is real and diagonal. Starting from Eq. (1), the S-matrix autocorrelation function (or "two-point function")

$$C_{ab}^{(2)}(\varepsilon) = \overline{S_{ab}^{\rm fl}(E-\varepsilon/2)S_{ab}^{\rm fl*}(E+\varepsilon/2)} \tag{4}$$

has been calculated analytically [1] for $N \gg 1$ and fixed Λ. The resulting expression depends only on the difference ε of the two energy arguments, on the average level spacing d of the system, and on the transmission coefficients T_a of all channels a defined by

$$T_a = 1 - |\overline{S_{aa}}|^2 \ . \tag{5}$$

The transmission coefficients obey $0 \le T_a \le 1$. These coefficients measure the unitarity deficit of the average S-matrix and give the probability with which the resonances take part in the reaction. This is seen by using the decomposition Eq. (3) and the definition Eq. (5) to write the unitarity condition for S in the form

$$T_a = \sum_b |S_{ab}^{\rm fl}(E)|^2 \ . \tag{6}$$

For $T_a = 0$ or $|\overline{S_{aa}}| = 1$, we have $S_{ab}^{\rm fl}(E) = 0$ for all b, and the resonances are not reached from channel a. Conversely, $\sum_b |S_{ab}^{\rm fl}(E)|^2$ is maximal for $T_a = 1$ or $\overline{S_{aa}} = 0$ (complete absorption of the incident flux in channel a by resonance formation). The transmission coefficients T_a determine the average width Γ of the resonances. An approximation for Γ is the "Weisskopf estimate"

$$\Gamma = \frac{d}{2\pi} \sum_a T_a \ . \tag{7}$$

The case of strongly overlapping resonances $\Gamma \gg d$ ("Ericson regime" [9, 10, 11]) occurs for $\sum_a T_a \gg 1$: The number Λ of channels must be large and most of the individual transmission coefficients T_a must not be small. Conversely, the case of nearly isolated resonances $\Gamma \ll d$ is realized when Λ is of order unity or when Λ is large but all T_a are small. The theory developed in Ref. [1] and used in Refs. [4, 5] applies to all values of Γ/d. Equation (7) is exact in the Ericson regime and fairly reliable elsewhere.

Under omission of kinematical factors the cross section in nuclear physics, the conductance in electron transport and the transmitted power in microwave billiards are all given by $|S_{ab}(E)|^2$ or by a sum of such terms. For brevity we refer to $|S_{ab}(E)|^2$ as to the cross section. The average cross section $\overline{|S_{ab}(E)|^2} = |\overline{S_{aa}(E)}|^2\delta_{ab} + \overline{|S_{ab}^{\rm fl}(E)|^2}$ is given in terms of $\overline{S_{aa}}$ and of $C_{ab}^{(2)}(0)$ and is, thus, known. Fluctuations of the cross section are measured in terms of the cross-section autocorrelation function

$$\mathcal{C}_{ab}(\varepsilon) = \overline{|S_{ab}(E+\varepsilon/2)|^2|S_{ab}(E-\varepsilon/2)|^2} - \overline{|S_{ab}|^2}^2 \ . \tag{8}$$

That function is the object of central interest in the present paper. With the help of the decomposition Eq. (3) we write

$$\begin{aligned}\mathcal{C}_{ab}(\varepsilon) = 2\delta_{ab}\mathfrak{Re}\Big\{ & \overline{S_{aa}}^2 C_{aa}^{(2)}(\varepsilon) \\ & + \overline{S_{aa}}\ \overline{S_{aa}^{\rm fl*}(E+\varepsilon/2)|S_{aa}^{\rm fl}(E-\varepsilon/2)|^2} \\ & + \overline{S_{aa}}\ \overline{S_{aa}^{\rm fl*}(E-\varepsilon/2)|S_{aa}^{\rm fl}(E+\varepsilon/2)|^2}\Big\} \\ & + \overline{|S_{ab}^{\rm fl}(E+\varepsilon/2)|^2|S_{ab}^{\rm fl}(E-\varepsilon/2)|^2} - \overline{|S_{ab}^{\rm fl}|^2}^2 \ . \end{aligned} \tag{9}$$

We have used that in the experiments and in the considered S-matrix model (Eq. (1)) $\overline{S_{aa}}$ is real, that by definition $\overline{S_{ab}^{\rm fl}(E)} = 0$ and that $\overline{S_{ab}^{\rm fl}(E_1)S_{ab}^{\rm fl}(E_2)} = 0$ for all a, b and all E_1, E_2. The last relation holds because all poles of S lie in the lower half of the complex energy plane. To determine $\mathcal{C}_{ab}(\varepsilon)$ we need to know the four-point function

$$C_{ab}^{(4)}(\varepsilon) = \overline{|S_{ab}^{\rm fl}(E+\varepsilon/2)|^2|S_{ab}^{\rm fl}(E-\varepsilon/2)|^2} - \overline{|S_{ab}^{\rm fl}|^2}^2 \tag{10}$$

and, in the elastic case $a = b$, also the three-point function

$$C_{ab}^{(3)}(\varepsilon) = \overline{S_{ab}^{\rm fl*}(E+\varepsilon/2)|S_{ab}^{\rm fl}(E-\varepsilon/2)|^2} \ . \tag{11}$$

These functions are known analytically only for $\varepsilon = 0$ and in the Ericson regime ($\Gamma \gg d$), see below.

To determine magnitude and ε-dependence of $\mathcal{C}_{ab}(\varepsilon)$, we combine analytical results with numerical and experimental evidence as follows. (i) Analytical results: In Refs. [4, 5] analytic expressions are given for two functions $F_{ab}^{(4)}(\varepsilon)$ and $F_{ab}^{(3)}(\varepsilon)$ that look similar to but actually differ from $C_{ab}^{(4)}(\varepsilon)$ and $C_{ab}^{(3)}(\varepsilon)$, respectively. These are defined by

$$\begin{aligned} F_{ab}^{(4)}(\varepsilon) &= \overline{\left[S_{ab}^{\rm fl*}(E+\varepsilon/2)\right]^2 \left[S_{ab}^{\rm fl}(E-\varepsilon/2)\right]^2} \ , \\ F_{ab}^{(3)}(\varepsilon) &= \overline{S_{ab}^{\rm fl*}(E+\varepsilon/2)\left[S_{ab}^{\rm fl}(E-\varepsilon/2)\right]^2} . \end{aligned} \tag{12}$$

We note that in $C_{ab}^{(4)}(\varepsilon)$ and in $C_{ab}^{(3)}(\varepsilon)$ the elements $S_{ab}^{\rm fl}$ and $S_{ab}^{\rm fl*}$ carry pairwise the same energy arguments. This is not the case for $F_{ab}^{(4)}(\varepsilon)$ and $F_{ab}^{(3)}(\varepsilon)$. However, $F_{ab}^{(3)}(0)$ coincides with $C_{ab}^{(3)}(0)$, and $F_{ab}^{(4)}(0)$ differs from $C_{ab}^{(4)}(0)$ only by the known term $\overline{|S_{ab}^{\rm fl}|^2}^2$. We are going to show

that for $\varepsilon \neq 0$ it is possible to approximate $C^{(4)}_{ab}(\varepsilon)$ in terms of $F^{(4)}_{ab}(\varepsilon)$, and under certain conditions $C^{(3)}_{ab}(\varepsilon)$ in terms of $F^{(3)}_{ab}(\varepsilon)$. For the convenience of the reader we, therefore, give in the Appendix analytic expressions for $F^{(n)}_{ab}(\varepsilon)$ for $n = 2, 3, 4$, where $F^{(2)}_{ab}(\varepsilon) \equiv C^{(2)}_{ab}(\varepsilon)$. We briefly show how the threefold integrals can be evaluated numerically to avoid the apparent singularities of the integrand. (ii) Numerical results: For the numerical simulations we use Eqs. (1) and (2) and fixed values for λ, for the transmission coefficients T_a, and for N as initial values. Calculations were typically done for several 100 realizations to minimize statistical errors. The results agree very well with the available analytical results but go beyond them. (iii) Data: The data stem from measurements of transmission and reflection amplitudes of microwaves in a flat cylindrical resonator made of copper and coupled to two antennas, see Refs. [3, 6]. Microwave power was coupled into the resonator with the help of a vector network analyzer. The range of the excitation frequency was chosen such that only one vertical electric field mode is excited. Then the microwave cavity simulates a two-dimensional quantum billiard [12, 13]. The resonator had the shape of a tilted stadium billiard whose classical dynamics is chaotic. Transmission and reflection amplitudes correspond to complex S-matrix elements that are theoretically modeled by Eqs. (1) and (2) [3, 6].

3. Inelastic case ($a \neq b$)

The inelastic case is simpler than the elastic one because it involves only the function $C^{(4)}_{ab}(\varepsilon)$, see Eq. (9). We begin with the Ericson regime $\Gamma \gg d$, see Refs. [9, 10, 11]. In Ref. [11] it was suggested and in Ref. [15] it was shown that for $\Gamma \gg d$ the fluctuating S-matrix elements $S^{\rm fl}_{ab}$ possess a bivariate Gaussian distribution centered at zero. That fact implies that all higher moments and correlation functions can be computed from $C^{(2)}_{ab}(\varepsilon)$ by way of Wick contraction. Hence $C^{(3)}_{ab}(\varepsilon) = 0$ and

$$C^{(4)}_{ab}(\varepsilon) = |C^{(2)}_{ab}(\varepsilon)|^2 \ . \qquad (13)$$

In the Ericson regime, the two-point function has the value [9, 15]

$$C^{(2)}_{ab}(\varepsilon) = (1 + \delta_{ab}) \ \frac{T_a T_b}{\sum_c T_c + 2i\pi\varepsilon/d} \ . \qquad (14)$$

Thus, for $a \neq b$ and $\Gamma \gg d$, the cross-section autocorrelation function is known analytically. It has the shape of a Lorentzian with width Γ as given by Eq. (7).

How far can we use Eq. (13) outside the Ericson regime, i.e., for smaller values of Γ/d? Figure 1 shows the ratio $C^{(4)}_{12}(0)/|C^{(2)}_{12}(0)|^2$ versus Γ/d as a function of Γ/d on a semi–logarithmic plot for three cases as indicated in the figure caption. Case (i) with unequal transmission coefficients is obtained from experimental data and suggests that Eq. (13) holds approximately for $\Gamma \gtrsim d$. The two other cases result from numerical simulations with, respectively, $\Lambda = 32$ and $\Lambda = 52$ equal transmission coefficients and imply, that Eq. (13) holds for $\Gamma \gtrsim 3d$. The ratio $C^{(4)}_{12}(0)/|C^{(2)}_{12}(0)|^2$ increases dramatically with decreasing Γ/d so that Eq. (13) cannot be used much below $\Gamma \approx d$.

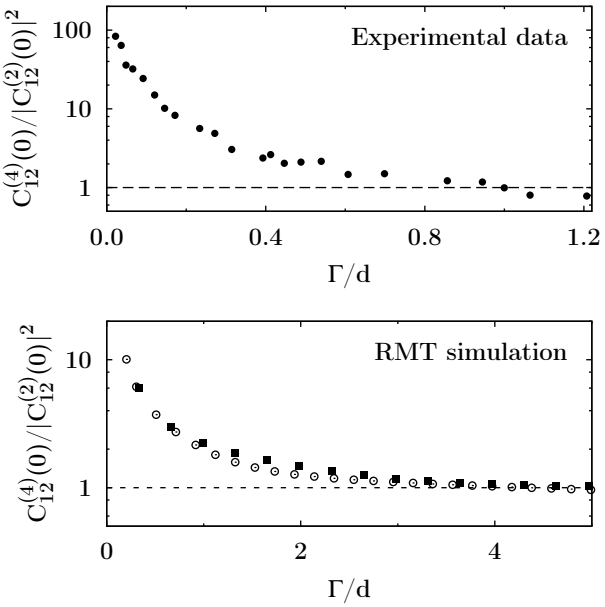

Figure 1: Ratios of four-point- and squared two-point-functions of $S^{\rm fl}_{12}$ on a semi-logarithmic plot for three cases. Upper panel: Experimental data [3, 6] (filled circles). Lower panel: Data generated numerically from Eq. (1) for $\Lambda = 32$ channels (open circles) and for $\Lambda = 52$ channels (full squares) with identical transmission coefficients.

The origin of the failure of Eq. (13) for small values of Γ/d is easily understood. Qualitatively speaking, it is intuitively clear that cross-section fluctuations (measured in units of the average cross section) are much larger for isolated than for overlapping resonances. Quantitatively, the assumption that underlies Eq. (13) is that the distribution of the fluctuating S-matrix elements $S^{\rm fl}_{ab}(E)$ is Gaussian. That assumption holds only if the width γ of the distribution is sufficiently small. Indeed, the unitarity condition Eq. (6) implies that for all a and b we must have $|S^{\rm fl}_{ab}|^2 \leq T_a \leq 1$, and γ must be so small that the contribution of the tails of the distribution that extend beyond the values $\pm T_a^{1/2}$, is negligible. Otherwise, significant deviations from a Gaussian distribution are to be expected. To estimate γ in the Ericson regime we use Eq. (14) which for $a \neq b$ gives $\gamma = |C^{(2)}_{ab}(0)|^{1/2} = [T_a T_b / \sum_c T_c]^{1/2}$. Thus, since $\sum_c T_c \gg 1$ this estimate yields $\gamma \ll 1$ as expected. For smaller values of Γ/d, constraints on the distribution of $S^{\rm fl}_{ab}$ due to the unitarity condition (6) are expected to become increasingly important as the number Λ of terms in the sum in Eq. (6) decreases.

We have checked this explanation by investigating the distribution of $S^{\rm fl}_{12}$. A bivariate Gaussian distribution for $S^{\rm fl}_{12}$ implies that the distribution of $z = |S^{\rm fl}_{12}|/\overline{|S^{\rm fl}_{12}|}$ has the

form $P(z) = (\pi/2)z\exp[-(\pi/4)z^2]$, and that the phase of $S_{12}^{\rm fl}$ is distributed uniformly in the interval $\{0, 2\pi\}$. In Fig. 2 and Fig. 3 and for values of Γ/d indicated above each panel, we compare in the upper row the function $P(z)$ with experimental and numerical data, respectively. In the panels in the lower row, we show the corresponding distributions of the phase. The numerical data in the three panels of Fig. 2 are obtained by simulating absorption in the resonator in terms of a large number of fictitious channels with small transmission coefficients in each channel. Then their sum τ is the only parameter. It was determined as described in [3] from a fit of the experimental autocorrelation function to the analytic result given in [1]. The data show that agreement with the bivariate Gaussian distribution is attained for $\Gamma/d \gtrsim 1$. The data in Fig. 3 (generated numerically for 32 equal channels) show agreement with the bivariate Gaussian distribution only for $\Gamma/d \gtrsim 3$. This suggests that the limit of a bivariate Gaussian distribution for $S_{ab}^{\rm fl}$ with $a \neq b$ is attained for larger values of Γ/d when all transmission coefficients are equal than when the transmission coefficients differ. These results account for the deviations from Eq. (13) displayed in Fig. 1.

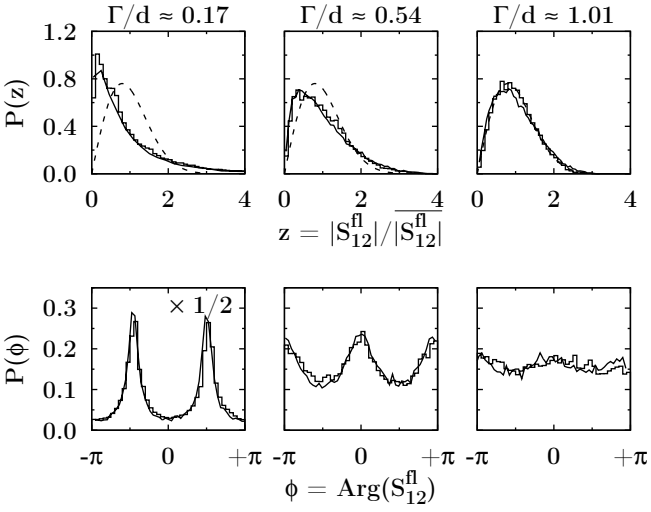

Figure 2: Distribution of the modulus (upper row) and phase (lower row) of $S_{12}^{\rm fl}$ obtained from the experimental data (histograms) and from numerical simulations (solid lines) for three values of Γ/d. In the upper row, the bivariate Gaussian distribution expected in the Ericson limit is shown as a dashed line. The transmission coefficients have the following values [3, 6]. For $\Gamma/d = 0.17$: $T_1 = 0.097$, $T_2 = 0.130$, $\tau_{\rm abs} = 0.810$, for $\Gamma/d = 0.54$: $T_1 = 0.417$, $T_2 = 0.475, \tau_{\rm abs} = 2.274$, for $\Gamma/d = 1.01$: $T_1 = 0.784$, $T_2 = 0.665, \tau_{\rm abs} = 4.903$.

Concerning the ε-dependence of $C_{12}^{(4)}(\varepsilon)$ and of $|C_{12}^{(2)}(\varepsilon)|^2$, our data show that for those values of Γ/d where the ratio $C_{12}^{(4)}(0)/|C_{12}^{(2)}(0)|^2 \approx 1$, that dependence is sufficiently similar so that $C_{12}^{(4)}(\varepsilon)$ can be reliably approximated by $|C_{12}^{(2)}(\varepsilon)|^2$. (By that we mean that the full two–point function defined in Eq. (4) and not the approximate form Eq. (14) has to be used). That leaves us with the question how to approximate $C_{12}^{(4)}(\varepsilon)$ analytically for $\Gamma \lesssim d$.

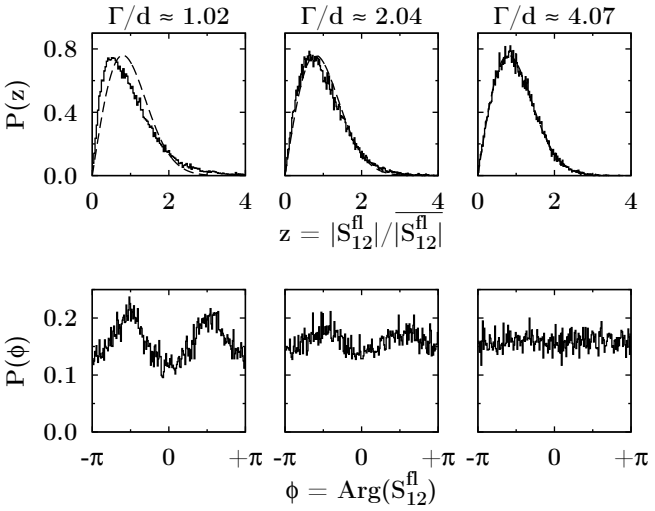

Figure 3: Distribution of the modulus (upper row) and phase (lower row) of $S_{12}^{\rm fl}$ obtained from numerical simulations (histograms) for $\Lambda = 32$ channels with identical transmission coefficients for three values of Γ/d. In the upper row, the bivariate Gaussian distribution expected in the Ericson limit is shown as a dashed line.

An obvious possibility is offered by the function $F_{12}^{(4)}(\varepsilon)$ defined in the first of Eqs. (12). Figure 4 shows experimental (upper two panels) and numerically (lowest panel) generated values of $|F_{12}^{(4)}(\varepsilon)|$ and of $C_{12}^{(4)}(\varepsilon)$ versus ε for two different values of Γ/d, and for $\Lambda = 32$ channels with identical transmission coefficients $T_a = 0.2$ and a value of Γ/d close to the largest achieved in the experiment, respectively. The function $|F_{12}^{(4)}(\varepsilon)|$ was rescaled so that at $\varepsilon = 0$ it agrees with $C_{12}^{(4)}(0)$. In the upper two panels the experimental curves for $C_{12}^{(4)}(\varepsilon)$ (filled circles) and the rescaled function $|F_{12}^{(4)}(\varepsilon)|$ are shown together with the analytic result for $|F_{12}^{(4)}(\varepsilon)|$ multiplied with the same scaling factor as the experimental one. In the lowest panel we compare the numerical result for $C_{12}^{(4)}(\varepsilon)$ with the analytic rescaled result for $|F_{12}^{(4)}(\varepsilon)|$. We note that the agreement is excellent for all three cases. Similarly good agreement was found also for $\Lambda = 52$ channels and several values of Γ/d. We conclude that we have reached a simple and reliable prescription for approximating $C_{12}^{(4)}(\varepsilon)$ analytically for all values of Γ/d: Calculate $C_{12}^{(4)}(0)$ and $|F_{12}^{(4)}(\varepsilon)|$ analytically. (The formulas needed [4, 5] are given in the Appendix). Rescale $|F_{12}^{(4)}(\varepsilon)|$ so that its value at $\varepsilon = 0$ agrees with $C_{12}^{(4)}(0)$. The resulting rescaled function $|F_{12}^{(4)}(\varepsilon)|$ is an excellent approximation to $C_{12}^{(4)}(\varepsilon)$ for all values of Γ/d.

4. Elastic Case ($a = b$)

The elastic case is analogous to the inelastic one only if $\overline{S_{aa}} = 0$. Then all conclusions drawn in Section 3 apply. In general, that is not the case. In particular, for $\Gamma \ll d$ (isolated resonances) the last term in Eq. (1) tends to zero and $\overline{S_{aa}}$ approaches unity. The unitarity constraint

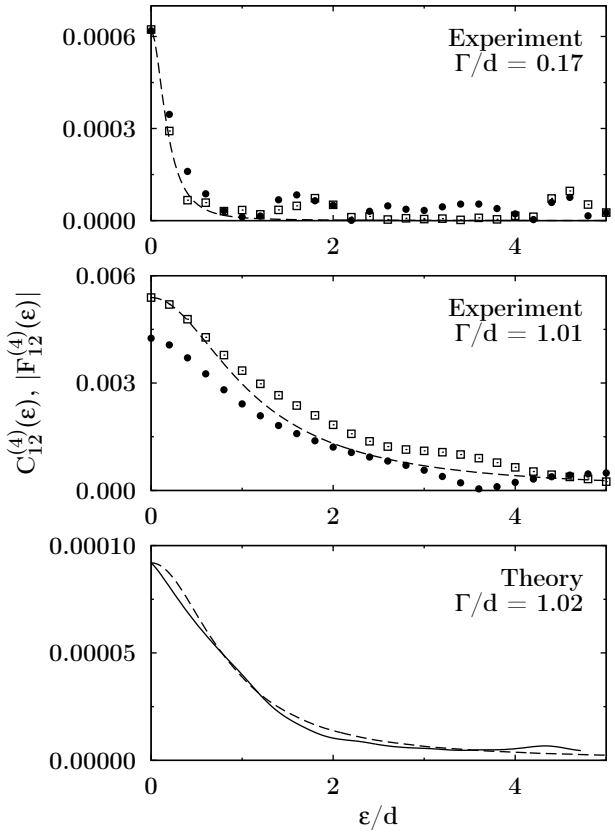

Figure 4: The dependence on ε of $C_{12}^{(4)}(\varepsilon)$ and of the renormalized function $|F_{12}^{(4)}(\varepsilon)|$ for three cases with Γ/d as indicated in the panels. In the upper two panels we show experimental curves for $C_{12}^{(4)}(\varepsilon)$ (filled circles) and for $|F_{12}^{(4)}(\varepsilon)|$ (open squares), in the lowest panel a numerically generated curve for $C_{12}^{(4)}(\varepsilon)$ (solid line) for 32 identical channels. In all three panels, the analytic function $|F_{12}^{(4)}(\varepsilon)|$ is shown as dashed line. Both the experimental and the analytic values for $|F_{12}^{(4)}(\varepsilon)|$ are renormalized with a factor determined from the analytic value for $C_{12}^{(4)}(0)$.

on S implies $|\overline{S_{aa}} + S_{aa}^{\rm fl}| \leq 1$ and the distribution of $S_{aa}^{\rm fl}$ must then become skewed. Therefore, we have to expect that Eq. (13) applies less generally in the elastic than in the inelastic case, and that $C_{aa}^{(3)}(\varepsilon)$ in Eq. (9) plays an important role. Actually, it was pointed out in Refs. [4, 5] that even in the Ericson limit, a profound difference between the elastic and the inelastic cases exists: For $\Gamma \gg d$, $\overline{|S_{aa}^{\rm fl}|^3}$ and $\overline{|S_{aa}^{\rm fl}|^4}$ have similar values unless $T_a \approx 1$ or $\overline{S_{aa}} \approx 0$. That shows that in order to predict $\mathcal{C}_{aa}(\varepsilon)$ we need to know both $C_{aa}^{(3)}(\varepsilon)$ and $C_{aa}^{(4)}(\varepsilon)$ for all values of Γ/d.

Concerning $C_{11}^{(4)}(0)$, we proceed as in Section 3 and display in Fig. 5 the ratio $C_{11}^{(4)}(0)/|C_{11}^{(2)}(0)|^2$ in the upper panel for experimental data, in the lower one for a numerical simulation with $\Lambda = 32$ equal transmission coefficients, as indicated in the figure caption. We reach the same conclusions as for $a \neq b$: When the transmission coefficients differ, the ratio is close to unity for $\Gamma \gtrsim d$, when they are equal for $\Gamma \gtrsim 3d$. As in the inelastic case, the reason for

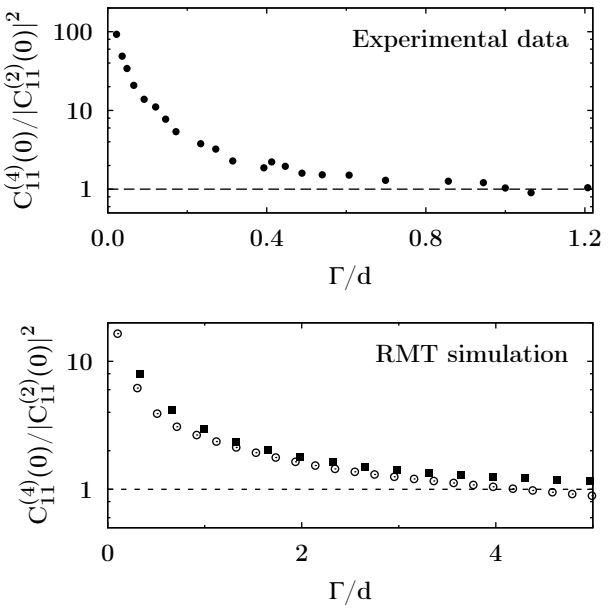

Figure 5: Same as Fig. 1 but for $S_{11}^{\rm fl}$.

the failure of Eq. (13) is the non–Gaussian distribution of $S^{\rm fl}$. This is shown in Figs. 6, 7. The deviations from a bivariate Gaussian distribution now occur for larger values of Γ/d than in the inelastic case, in keeping with the expectations formulated at the beginning of this Section.

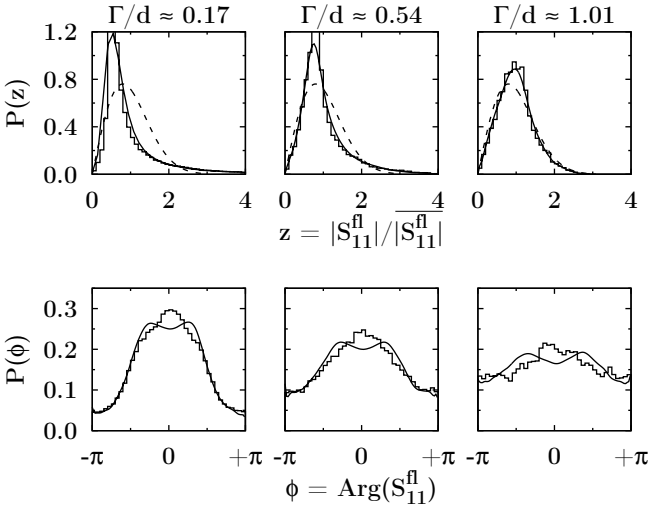

Figure 6: Same as Fig. 2 but for $S_{11}^{\rm fl}$.

In Fig. 8 we show that, as in the elastic case, the rescaled function $|F_{11}^{(4)}(\varepsilon)|$ agrees well with $C_{11}^{(4)}(\varepsilon)$ for all values of Γ/d. Such agreement was likewise found for the case of $\Lambda = 52$ channels with identical transmission coefficients. Figure 9 shows that the three-point function $\mathfrak{Re}\left(C_{11}^{(3)}(\varepsilon)\right)$ is approximated quite well by the (unrenormalized) function $\mathfrak{Re}\left(F_{11}^{(3)}(\varepsilon)\right)$ defined in the second of Eqs. (12) for the

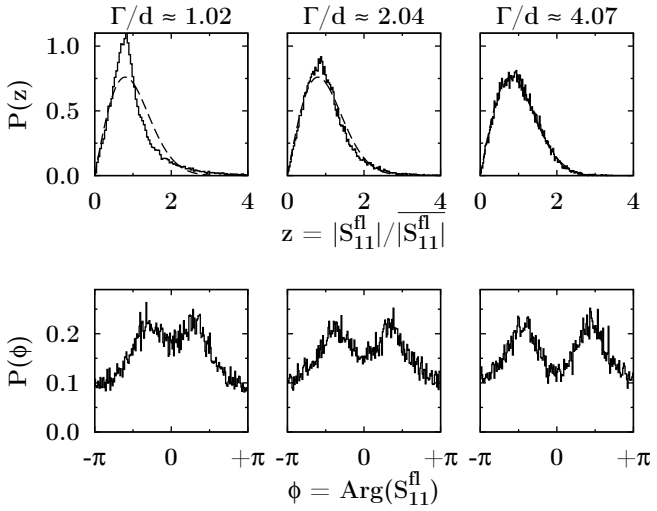

Figure 7: Same as Fig. 3 but for $S_{11}^{\rm fl}$.

experimental data with $\Gamma/d = 0.17$ (upper panel), where the resonances are nearly isolated, and for the numerical simulations with $\Lambda = 32$ identical transmission coefficients $T_a = 0.2$ (lower panel). However, considerable deviations are observed for the experimental data with $\Gamma/d = 1.01$ (middle panel). Thus, the conclusions drawn for the inelastic case apply similarly to the elastic one only in the regime of isolated resonances and the Ericson regime, where $\overline{S_{aa}}$ is vanishingly small. To obtain an analytic expression for the cross-section autocorrelation function we now need to replace $C_{11}^{(4)}(\varepsilon)$ with the rescaled function $|F_{11}^{(4)}(\varepsilon)|$ and the function $\mathfrak{Re}\left(C_{11}^{(3)}(\varepsilon)\right)$ with $\mathfrak{Re}\left(F_{11}^{(3)}(\varepsilon)\right)$. While the former replacement yields an excellent approximation for all values of Γ/d, this is not generally true for the latter in the intermediate regime of weakly overlapping resonances. Still, for the numerical simulations with $\Lambda = 32$ equal transmission coefficients $T_a = 0.2$, which corresponds to $\Gamma/d = 1.02$, the resulting analytic expression for the cross-section autocorrelation function yields a good approximation, because there both, the values of $\mathfrak{Re}\left(F_{11}^{(3)}(\varepsilon)\right)$ and of $\mathfrak{Re}\left(C_{11}^{(3)}(\varepsilon)\right)$, are negligibly small as compared to $\mathcal{C}_{ab}(\varepsilon)$, whereas this is not true for the experimental data with $\Gamma/d = 1.01$.

5. Summary

We return to the questions raised in the Introduction. We have shown that Eq. (13) holds essentially only in the Ericson regime and, for the elastic case, even there only approximately. This is because of the constraint imposed on the distribution of $S^{\rm fl}$ by unitarity. Hence, in the inelastic case the cross–section autocorrelation function can be reliably predicted from Eq. (13) for $\Gamma/d \gtrsim 1$ for inequivalent channels and for $\Gamma/d \gtrsim 3$ for identical channels. Even more stringent constraints exist in the elastic case. We

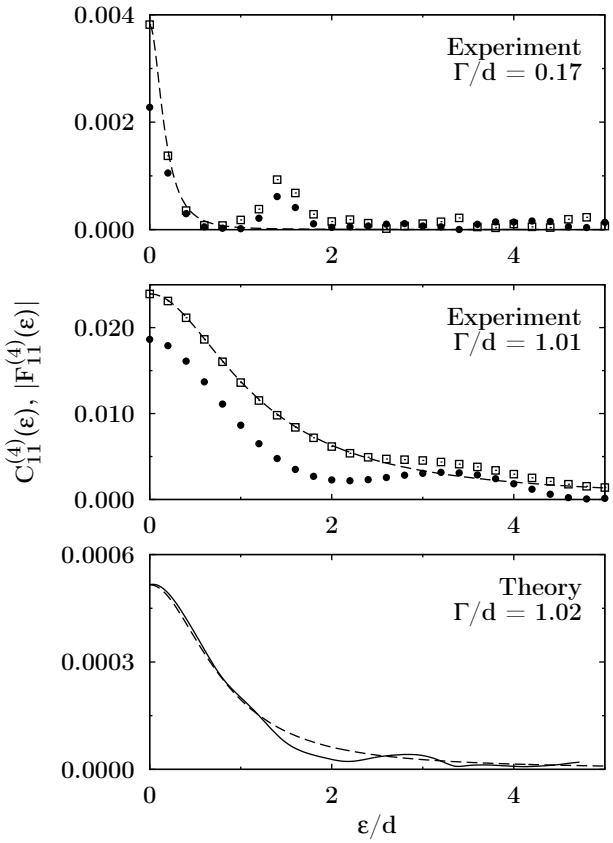

Figure 8: Same as Fig. 4 but for the elastic case.

have demonstrated, however, that for the inelastic case for all values of Γ/d and for the elastic case under certain conditions an excellent approximation to the cross-section autocorrelation function may be obtained by replacing in Eq. (9) the three-point function $C_{ab}^{(3)}(\varepsilon)$ by $F_{ab}^{(3)}(\varepsilon)$ and the four-point function $C_{ab}^{(4)}(\varepsilon)$ by the rescaled function $F_{ab}^{(4)}(\varepsilon)$. With these replacements, Eq. (9) takes the form

$$\begin{aligned}\mathcal{C}_{ab}(\varepsilon) &\simeq 2\delta_{ab}\mathfrak{Re}\Big\{\overline{S_{aa}}^2\, C_{aa}^{(2)}(\varepsilon) \\ &+ \overline{S_{aa}}\, F_{aa}^{(3)}(\varepsilon) + \overline{S_{aa}}\, F_{aa}^{(3)}(-\varepsilon)\Big\} \\ &+ \frac{C_{ab}^{(4)}(0)}{|F_{ab}^{(4)}(0)|}|F_{ab}^{(4)}(\varepsilon)| \ . \end{aligned} \tag{15}$$

The input parameters for the evaluation of Eq. (15) are the average S–matrix elements and the associated transmission coefficients for all channels and, for the dependence on ε, the average level spacing d of the scattering system. In terms of these parameters, the two–point function $C_{ab}^{(2)}(\varepsilon)$ is given in Ref. [1], and $C_{ab}^{(4)}(0)$ and the functions $F_{ab}^{(4)}(\varepsilon)$ and $F_{ab}^{(3)}(\varepsilon)$ in Refs. [4, 5]. For the convenience of the reader, all relevant formulas are collected in the Appendix in a form suitable for numerical implementation. For the elastic case, Eq. (15) provides an excellent approximation

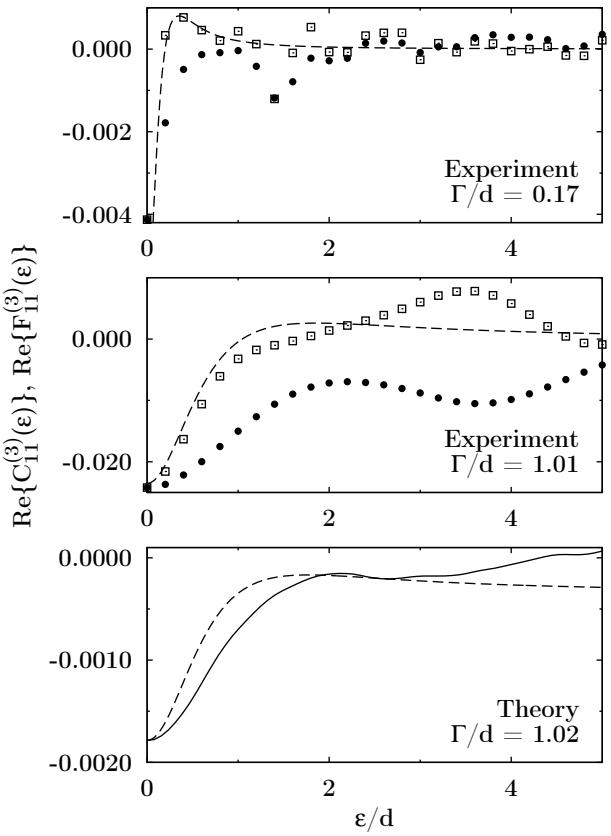

Figure 9: The dependence on ε of $\mathfrak{Re}\left(F_{11}^{(3)}(\varepsilon)\right)$ and of $\mathfrak{Re}\left(C_{11}^{(3)}(\varepsilon)\right)$ for three cases with Γ/d as indicated in the panels. In the upper two panels we show experimental curves for $\mathfrak{Re}\left(C_{11}^{(3)}(\varepsilon)\right)$ (filled circles) and for $\mathfrak{Re}\left(F_{11}^{(3)}(\varepsilon)\right)$ (open squares), in the lowest panel a numerically generated curve $\mathfrak{Re}\left(C_{11}^{(3)}(\varepsilon)\right)$ for 32 identical channels (solid line). The analytic function $\mathfrak{Re}\left(F_{11}^{(3)}(\varepsilon)\right)$ is shown as dashed line in all three panels. The limited accuracy of our comparison is indicated by the difference between the dashed line and the open squares in the upper two panels.

for the cross-section autocorrelation function for all values of Γ/d only for $\varepsilon = 0$. For $\varepsilon > 0$ Eq. (15) yields a good approximation in the regime of isolated and strongly overlapping resonances, whereas in the intermediate regime of weakly overlapping resonances this is true, if the contribution of $C_{ab}^{(3)}(\varepsilon)$ or equivalently of $|F_{ab}^{(3)}(\varepsilon)|$ to $\mathcal{C}_{ab}(\varepsilon)$ is negligible.

Acknowledgement

We thank T. Friedrich for a discussion at an early stage of this work. The research has been supported through the SFB 634 by the DFG.

Appendix

For the evaluation of $\mathcal{C}_{ab}(\varepsilon = 0)$ in terms of $S^{\rm fl}$ and $\overline{S}$ as given in Eq. (9) we need to compute $C_{ab}^{(2)}(\varepsilon = 0)$, $C_{aa}^{(3)}(\varepsilon = 0) = \overline{S_{ab}^{\rm fl*}(0)|S_{ab}^{\rm fl}(0)|^2}$ and $C_{ab}^{(4)}(\varepsilon = 0) = \overline{|S_{ab}^{\rm fl}(0)|^4} - \overline{|S_{ab}^{\rm fl}(0)|^2}^2$. The autocorrelation coefficient $C_{ab}^{(2)}(\varepsilon = 0)$, $\overline{S_{ab}^{\rm fl*}(0)|S_{ab}^{\rm fl}(0)|^2}$ and $\overline{|S_{ab}^{\rm fl}(0)|^4}$ are given in terms of a threefold integral, c.f. Refs. [1, 4],

$$F_{ab}^{(n)}(0) = \frac{1}{8}\int_0^\infty \mathrm{d}\lambda_1 \int_0^\infty \mathrm{d}\lambda_2 \int_0^1 \mathrm{d}\lambda\, \mathcal{J}(\lambda,\lambda_1,\lambda_2) \times \prod_c \frac{1-T_c\,\lambda}{\sqrt{(1+T_c\lambda_1)(1+T_c\,\lambda_2)}}\, \mathcal{F}_{ab}^{(n)}(\lambda,\lambda_1,\lambda_2) \tag{16}$$

where the integration measure is given as

$$\mathcal{J}(\lambda,\lambda_1,\lambda_2) = \frac{\lambda(1-\lambda)|\lambda_1-\lambda_2|}{(\lambda+\lambda_1)^2(\lambda+\lambda_2)^2\sqrt{\lambda_1(1+\lambda_1)\lambda_2(1+\lambda_2)}}\,. \tag{17}$$

For $n = 2$, i.e. for $\overline{|S_{ab}^{\rm fl}(0)|^2}$ the factor $\mathcal{F}(\lambda,\lambda_1,\lambda_2)$ equals

$$\begin{aligned}\mathcal{F}_{ab}^{(2)}(\lambda,\lambda_1,\lambda_2) = {} & \delta_{ab}\,|\overline{S_{aa}}|^2\,T_a^2\left(\frac{\lambda_1}{1+T_a\lambda_1}+\frac{\lambda_2}{1+T_a\lambda_2}+\frac{2\lambda}{1-T_a\lambda}\right)^2 \\ & + (1+\delta_{ab})\,T_aT_b\left(\frac{\lambda_1(1+\lambda_1)}{(1+T_a\lambda_1)(1+T_b\lambda_1)}\right. \\ & \left. + \frac{\lambda_2(1+\lambda_2)}{(1+T_a\lambda_2)(1+T_b\lambda_2)} + \frac{2\lambda(1-\lambda)}{(1-T_a\lambda)(1-T_b\lambda)}\right),\end{aligned} \tag{18}$$

for $n = 3$, i.e. for $\overline{S_{ab}^{\rm fl*}(0)|S_{ab}^{\rm fl}(0)|^2}$ it equals

$$\begin{aligned}\mathcal{F}_{ab}^{(3)}(\lambda,\lambda_1,\lambda_2) = {} & -\overline{S}_{aa}\Big(4\mathrm{trg}(\mu_a\nu_a)+2\mathrm{trg}(\mu_a)\mathrm{trg}(\nu_a) \\ & + r_a\left\{\mathrm{trg}\left(\mu_a^2\right)+\frac{1}{2}\left[\mathrm{trg}(\mu_a)\right]^2\right\}\Big)\delta_{ab}\end{aligned} \tag{19}$$

and for $n = 4$, i.e. for $\overline{|S_{ab}^{\rm fl}(0)|^4}$ we have

$$\begin{aligned}\mathcal{F}_{ab}^{(4)}(\lambda,\lambda_1,\lambda_2) = {} & \left\{\mathrm{trg}(\nu_a)+\frac{1}{2}r_a\left[\mathrm{trg}(\mu_a)\right]^2\right\} \\ & \times\left\{\mathrm{trg}(\nu_b)+\frac{1}{2}r_b\left[\mathrm{trg}(\mu_b)\right]^2\right\} \\ & + \delta_{ab}\Big(\left[\mathrm{trg}(\nu_a)\right]^2+4\mathrm{trg}\left(\nu_a^2\right) \\ & + r_a^2\mathrm{trg}\left(\mu_a^2\right)\left\{\mathrm{trg}\left(\mu_a^2\right)+\left[\mathrm{trg}(\mu_a)\right]^2\right\} \\ & + r_a\Big\{\left[\mathrm{trg}(\mu_a)\right]^2\mathrm{trg}(\nu_a) \\ & + 8\,\mathrm{trg}(\mu_a)\mathrm{trg}(\mu_a\nu_a)+8\,\mathrm{trg}\left(\mu_a^2\nu_a\right)\Big\}\Big).\end{aligned} \tag{20}$$

Here, $r_a = 1 - T_a$ and μ_a, ν_a are the matrices

$$\begin{aligned} \mu_a &= T_a\lambda_0 \left(1 + T_a\lambda_0\right)^{-1} , \\ \nu_a &= T_a^2\lambda_0(1+\lambda_0)\left(1 + T_a\lambda_0\right)^{-2} , \end{aligned} \tag{21}$$

where λ_0 is the 4×4 diagonal matrix with entries λ_1, λ_2, $-\lambda$ and $-\lambda$. For a 4×4 matrix M with diagonal elements m_{ii} the graded trace trg is defined as $\mathrm{trg}(M) = (m_{11} + m_{22}) - (m_{33} + m_{44})$. Analytic expressions for the functions $F_{ab}^{(3)}(\varepsilon)$ and $F_{ab}^{(4)}(\varepsilon)$ defined in Eqs. (12) are obtained by multiplying $\mathcal{F}_{ab}^{(2)}(\lambda, \lambda_1, \lambda_2)$ in Eq. (18) and $\mathcal{F}_{ab}^{(3)}(\lambda, \lambda_1, \lambda_2)$ in Eq. (19) and $\mathcal{F}_{ab}^{(4)}(\lambda, \lambda_1, \lambda_2)$ in Eq. (20) with the exponential

$$\exp\left[-i\left(\lambda_1 + \lambda_2 + 2\lambda\right)\pi\varepsilon/d\right] . \tag{22}$$

The integral Eq. (16) contains several singularities. These can be handled by proceeding as in Section 5 of Ref. [14]. We define the variable

$$p = \lambda_1 + \lambda_2 + 2\lambda \; . \tag{23}$$

Then the exponential in Eq. (22) turns into

$$\exp(-ip\pi\varepsilon/d) . \tag{24}$$

We distinguish the two cases $p \leq 2$ and $p > 2$. For $p \leq 2$ we define two further integration variables

$$s = \frac{\sqrt{\lambda_1 + \lambda}}{\sqrt{\lambda_1 + \lambda_2 + 2\lambda}} , \tag{25}$$

$$t = \frac{\sqrt{\lambda_1}}{\sqrt{\lambda_1 + \lambda}} . \tag{26}$$

For the inverse transformation that yields

$$\lambda = ps^2\left(1 - t^2\right) , \tag{27}$$

$$\lambda_1 = ps^2t^2 , \tag{28}$$

$$\lambda_2 = p\left(1 + s^2t^2 - 2s^2\right) . \tag{29}$$

The Jacobian for this transformation is equal to $4p^2s^3t$. The threefold integral in Eq. (16) becomes

$$\begin{aligned} &F_{ab}^{(n)}(\varepsilon)_{(p\leq 2)} = \\ &\int_0^2 \mathrm{d}p \int_0^{1/\sqrt{2}} \mathrm{d}s \int_0^1 \mathrm{d}t \, \frac{e^{-ip\pi\varepsilon/d}}{p\left(1-s^2\right)^2\sqrt{\left(1+ps^2t^2\right)}} \\ &\quad \times \frac{\left[1 - ps^2\left(1-t^2\right)\right]\left(1-2s^2\right)\left(1-t^2\right)}{\sqrt{\left(1+s^2t^2-2s^2\right)\left[1+p\left(1+s^2t^2-2s^2\right)\right]}} \\ &\quad \times \prod_c \frac{1 - T_c\,\lambda}{\sqrt{(1+T_c\lambda_1)(1+T_c\,\lambda_2)}}\, \mathcal{F}_{ab}^{(n)}(\lambda, \lambda_1, \lambda_2) . \end{aligned} \tag{30}$$

For $p > 2$ we define additional integration variables

$$s = \sqrt{\lambda_1 + \lambda} , \tag{31}$$

$$t = \frac{\sqrt{\lambda_1}}{\sqrt{\lambda_1 + \lambda}} . \tag{32}$$

For the inverse transformation that yields

$$\lambda = s^2\left(1 - t^2\right) , \tag{33}$$

$$\lambda_1 = s^2t^2 , \tag{34}$$

$$\lambda_2 = p + s^2t^2 - 2s^2 . \tag{35}$$

The Jacobian equals $4s^3t$ and the threefold integral in Eq. (16) becomes

$$\begin{aligned} &F_{ab}^{(n)}(\varepsilon)_{(p>2)} = \\ &\int_2^\infty \mathrm{d}p \int_0^{\sqrt{p/2}} \mathrm{d}s \int_{\sqrt{1-s^{-2}}\theta(s-1)}^1 \mathrm{d}t \, \frac{e^{-ip\pi\varepsilon/d}}{\left(p-s^2\right)^2} \\ &\quad \times \frac{\left[1 - s^2\left(1-t^2\right)\right]\left(p-2s^2\right)\left(1-t^2\right)}{\sqrt{\left(p+s^2t^2-2s^2\right)\left(1+s^2t^2\right)\left(1+p+s^2t^2-2s^2\right)}} \\ &\quad \times \prod_c \frac{1 - T_c\,\lambda}{\sqrt{(1+T_c\lambda_1)(1+T_c\,\lambda_2)}}\, \mathcal{F}_{ab}^{(n)}(\lambda, \lambda_1, \lambda_2) \end{aligned} \tag{36}$$

where the θ-function is defined by

$$\theta(x) = 0 \text{ for } x \leq 0 , \tag{37}$$

$$\theta(x) = 1 \text{ for } x > 0 . \tag{38}$$

References

[1] J. J. M. Verbaarschot, H. A. Weidenmüller, and M. R. Zirnbauer, Phys. Rep. **129** (1985) 367.
[2] C. W. Beenakker, Rev. Mod. Phys. **69** (1997) 731.
[3] B. Dietz, T. Friedrich, H. L. Harney, D.-M. Miski-Oglu, A. Richter, F. Schäfer, and H. A. Weidenmüller, Phys. Rev. E **78** (2008) 055204(R), and references therein.
[4] E. D. Davis and D. Boosé, Phys. Lett. **B 211** (1988) 379.
[5] E. D. Davis and D. Boosé, Z. Physik **A 332** (1989) 427.
[6] B. Dietz, T. Friedrich, H. L. Harney, D.-M. Miski-Oglu, A. Richter, F. Schäfer, J. Verbaarschot, and H. A. Weidenmüller, Phys. Rev. Lett. **103** (2009) 064101.
[7] C. Mahaux and H. A. Weidenmüller, *Shell-Model Approach to Nuclear Reactions*, North-Holland, Amsterdam (1969).
[8] C. Engelbrecht and H. A. Weidenmüller, Phys. Rev. **C 8** (1973) 859.
[9] T. Ericson, Phys. Rev. Lett. **5** (1960) 430.
[10] T. Ericson, Ann. Phys. (N.Y.) **23** (1963) 390.
[11] D. M. Brink and R. O. Stephen, Phys. Lett. **5** (1963) 77.
[12] H.-J. Stöckmann and J. Stein, Phys. Rev. Lett. **64** (1990) 2215.
[13] H.-D. Gräf, H. L. Harney, H. Lengeler, C. H. Lewenkopf, C. Rangacharyulu, A. Richter, P. Schardt, and H. A. Weidenmüller, Phys. Rev. Lett. **69** (1992) 1296.
[14] J. J. M. Verbaarschot, Ann. Phys. (N.Y.) **168** (1986) 368.
[15] D. Agassi, H. A. Weidenmüller, and G. Mantzouranis, Phys. Rep. **22** (1975) 145.